University of Szeged

Faculty of Pharmacy

Institute of Pharmaceutical Technology and Regulatory Affairs

Summary of Ph.D. thesis

DEVELOPMENT OF ISONIAZID LOADED NANOTECHNOLOGY-BASED DRY POWDER PULMONARY FORMULATIONS FOR TREATMENT OF TUBERCULOSIS

By

Mahwash Mukhtar

Pharm. D., M.Phil.

Supervisor:

Dr. habil. Rita Ambrus *PhD*

SZEGED

2022

University of Szeged

Doctoral School of Pharmaceutical Sciences
Head: Prof. Dr. Judit Hohmann D.Sc

Educational Program: Pharmaceutical Technology
Head: Prof. Dr. Ildikó Csóka Ph.D.

Institute of Pharmaceutical Technology and Regulatory Affairs
Supervisor: Dr. habil Rita Ambrus Ph.D.

Mahwash Mukhtar

DEVELOPMENT OF ISONIAZID LOADED NANOTECHNOLOGY-BASED DRY POWDER PULMONARY FORMULATIONS AS TREATMENT APPROACHES FOR TUBERCULOSIS

Complex Exam Committee:

Head: Prof. Dr. Piroska Szabó-Révész D.Sc., Institute of Pharmaceutical Technology and Regulatory Affairs, University of Szeged

Members: Prof. Dr. Ildikó Bácskay Ph.D., Department of Pharmaceutical Technology, University of Debrecen

Dr. habil Zoltán Aigner Ph.D., Institute of Pharmaceutical Technology and Regulatory Affairs, University of Szeged

Reviewer Committee:

Head: Prof. Dr. István Zupkó, DSc., University of Szeged, Faculty of Pharmacy Institute of Pharmacodynamics and Biopharmacy

Reviewers: Prof. Bissera Pilicheva, Associate Prof. Department of Pharmaceutical Sciences, Medical University of Plovdiv, Bulgaria

Dr. László Janovák PhD, University of Szeged Faculty of Science and Informatics, Department of Physical Chemistry and Materials Science

Members: Dr. Eszter Ducza, PhD, University of Szeged, Faculty of Pharmacy Institute of Pharmacodynamics and Biopharmacy

Dr. Péter Doró, PhD, University of Szeged, Faculty of Pharmacy Department of Clinical Pharmacy

SZEGED

2022

1. INTRODUCTION

Tuberculosis (TB) remains an epidemic in this scientifically advanced world. According to a statistical survey by the world health organization (WHO), TB is the leading cause of death of over 1.5 million people annually across the globe. It is caused by Mycobacterium tuberculosis (M.Tb) which enters the lungs via inhalation and is phagocytosed by alveolar macrophages (AM) and then resides in the AM. M.Tb interacts with the T-lymphocytes to differentiate macrophages into granulomas characterized by the infiltration of inflammatory mononuclear cells. Later, the T-lymphocytes (effector cells) produce cytokines to facilitate the activation of previously infected macrophages to kill the M.Tb residing inside. Hence, T-cell response and activation are essential to the immune regulation in TB. The ineffective treatment is unable to eradicate the primary TB infection in the lungs which can then disseminate into the other organs leading to miliary TB.

Numerous drug delivery routes have been explored for drug delivery in TB. Currently, pulmonary drug delivery is gaining interest for the treatment of intra- and extra-pulmonary diseases. The advantage of pulmonary delivery is attributed to its high vascularization, avoidance of first-pass metabolism, and henceforth maintenance of therapeutic levels of the drug in the lungs. The use of dry powders for inhalation (DPIs) offers high formulation stability and deep lung deposition. Over the past decade, the use of nanotechnology in the pharmaceutical sciences has received attention due to improved physicochemical properties, enhanced cellular uptake, and improved retention and penetration. Moreover, the nanostructures can also be exploited for targeted delivery of drugs to a specific organ with minimal off-site toxicity.

Recently, the potential of nanotechnology in the DPIs is being studied to combine the benefits of nanoscale formulation and the localized effect of DPIs. Drug delivery by nano-based DPIs can improve the fine particle fraction (FPF) of inhaled powder, mass median aerodynamic diameter (MMAD), lung retention, drug release profile, cellular uptake, immune response, and sufficient availability of the drug in the deeper tissues of the lung. The fabrication of a favorable pulmonary DPI system with suitable composition is thereof desired for the treatment of TB. Development of the rational patient-friendly pharmaceutical dosage form is the time taking and extensive work. However, the quality by design (QbD) method is a systematic approach and effective application that takes into consideration every aspect of product quality attributes during the early stage of dosage development whereas the design of experiment (DoE) facilitates the optimization of a pharmaceutical formulation.

Abbreviations:

ACI–Andersen cascade impactor; AM–Alveolar macrophages; CMAs–Critical material attributes; CQAs–Critical quality attributes; CPPs–Critical process parameters; CS–Chitosan; DMEM–Dulbecco's modified Eagle's medium; DOE–Design of experiment; DPI–Dry powder for inhalation; DSC–Differential Scanning Calorimetry; EDAC–(1-ethyl-3-3(3-dimethylamino propyl) carbodiimide hydrochloride)); EE–Encapsulation efficiency; FDA–U.S. Food and Drug Administration; FTIR–Fourier transform infrared spectroscopy; EMA–European Medicines Agency; FPF–Fine particle fraction; HA–Hyaluronic acid; IDO–2,3-Indoleamine dioxygenase; INH–Isoniazid; I400–InhaLac® 400; MC–Mannosylated chitosan; MMAD–Mass median aerodynamic diameter; M.Tb–Mycobacterium tuberculosis; NGI–Next-generation impactor; PDI–Polydispersity index; QbD–Quality by design; QTPP–Quality target product profile; Rh-B–Rhodamine-B; RPMI-1640–Roswell Park Memorial Institute medium; TB–Tuberculosis; TGA–Thioglycolic acid; TPP–Sodium tri-polyphosphate; WHO–World health organization.; XRPD–X-ray Powder Diffraction

2. AIMS OF THE WORK

The major aim of this Ph.D. work was to develop and investigate the anti-tubercular isoniazid (INH) loaded nanotechnology-based DPIs for targeted drug delivery. Macrophage targeting is favorable to eradicate the TB infection, therefore, the polymers were chosen for their affinity towards the surface receptors of macrophages.

This Ph.D. work was designed and studied in the following parts, following the step-by-step approach:

1. Literature review about the pulmonary drug delivery systems for treatment of TB.
2. Use of different polymers such as chitosan (CS) and mannosylated chitosan (MC) along with hyaluronic acid (HA) to design the different hybrid INH loaded nanopowders to target the AM in lungs for the effective treatment of TB.
3. Application of the cost-effective ionic gelation method for the preparation of nanosuspensions based on DoE. Studying drying methods to obtain dry powders (spray-drying and freeze-drying).
4. Structural and morphological examination of the developed nanosystems along with physicochemical characterization through different *in vitro* techniques. Moreover, the *in silico* studies were also performed to evaluate the deposition profile of nanopowders in the lungs.
5. *Ex vivo* studies on the different cell lines to demonstrate the behavior of nanopowders in terms of toxicity, immune-regulation, and tolerogenic effects, particularly on human-derived macrophages.

3. MATERIALS AND METHODS

3.1. Materials

3.1.1. Active pharmaceutical ingredient

Isoniazid was purchased from Pannon Pharma Kft (Hungary). Hyaluronic acid was provided by Contipro Biotech (Czech Republic).

3.1.2. Excipients

Different polymers and excipients were employed to obtain the nanopowders. Chitosan [75–85 % deacetylated, low molecular weight, 50-190 kDa, Poly (D-glucosamine)] and trehalose were obtained from Sigma-Aldrich (MO, USA). Sodium tri-polyphosphate was purchased from Alfa Aesar (ThermoFischer, Germany). Mannitol and InhaLac® 400 (I400) were provided by MEGGLE Group, (Wasserburg, Germany). D-mannose was purchased from Sigma-Aldrich Chemie GmbH, (Steinheim, Germany).

3.1.3. Cell lines and media

Macrophage Raw 264.7 and A549 cell lines were purchased from ATCC (VA, USA). Roswell Park Memorial Institute medium (RPMI-1640) and Dulbecco's modified Eagle's medium (DMEM) were

bought from GIBCO® (ThermoFischer Scientific, MA, USA). Ficoll-Paque TM PLUS (density 1.077 g/ml) was purchased from GE Healthcare Bioscience AB (IL, USA). Phycoerythrin-conjugated anti-human CD80 (CD80-PE) and Allophycocyanin-conjugated anti-human CD83 (CD83-APC) were obtained from Miltenyi Biotec (Bergisch Gladbach, Germany).

3.2. Methods

3.2.1. Synthesis of polymer

Thioglycolic acid (TGA) was poured into the 1 % CS solution in acetic acid. After subsequent addition of 50 mM EDAC (1-ethyl-3-3(3-dimethylamino propyl) carbodiimide hydrochloride)) to activate carboxylic groups of TGA, an amide linkage between CS and TGA was developed. The polymeric suspension of thiolated chitosan was obtained which was then conjugated with mannose to obtain MC. For this purpose, 0.12 M cyanoborohydride was added to the 2 % thiolated chitosan suspension (in acetic acid) to facilitate the reductive amination (**Figure 1**). Following, 0.33 M D-mannose was added to the suspension with continuous stirring. The pink polymeric suspension of MC was acquired.

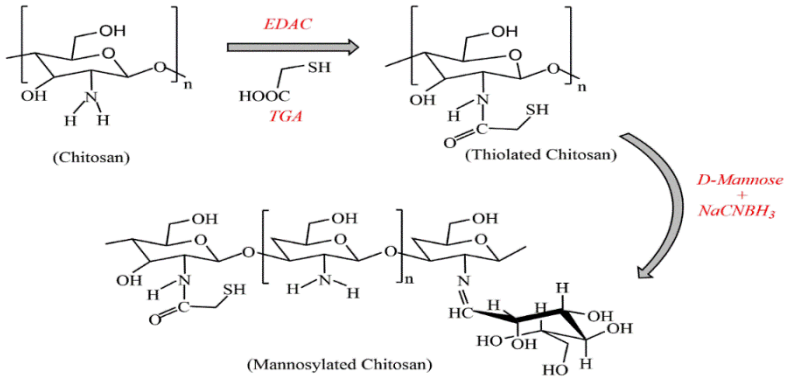

Figure 1: *The schematic pathway for the synthesis of mannosylated chitosan.*

3.2.2. Determination of QbD elements and application of DoE

Lean QBD software® (QBD works LLC, Fremont, USA) was used to illustrate the risk assessment and interdependence between quality target product profile (QTPPs) and critical quality attributes (CQAs); and between CQAs and critical material attributes (CMAs)/critical process parameters (CPPs). The variables for the screening DoE were selected based on risk assessment. For this work, Box-Behnken was chosen to take into consideration the various variables simultaneously to save time and resources. The independent factors chosen through risk assessment were the concentration of HA (X_1, lower limit: 2.5 mg, upper limit 6.5 mg), the concentration of CS (X_2, lower limit: 1.25 mg, upper limit 3.25 mg), and sonication pulse ratio (X_3, lower limit: 30, upper limit 50). On the other hand, 3 dependent or response variables were selected (Y_1: size, Y_2: polydispersity index (PDI), Y_3: zeta potential). A set of experimental runs was generated by STATISTICA® 10 software that used ANOVA for statistical significance ($p < 0.05$).

3.2.3. Preparation of nanosuspensions

To obtain the nanosuspensions, an ionic gelation method was employed by using cross-linker Sodium tri-polyphosphate (TPP). Polymers, CS was solubilized in 0.5 M Glacial acetic acid. The pH of the polymeric system was maintained at 4.9. Similarly, HA was dissolved in double distilled water to obtain a polymeric suspension. TPP (0.5-2 mg/ml) was added dropwise to the CS suspension until the appearance of a bluish haze followed by the addition of HA suspension under probe sonicator. 10 mg of INH (10 % of oral dose) solubilized in 1 ml methanol was injected into the prepared nanosuspension to obtain INH loaded CS and HA NPs (INH-CS/HA NPs). A similar protocol was used to prepare the INH-loaded MC and HA hybrid NPs (INH-MC/HA NPs).

3.2.4. Preparation of dry powders

The nanosuspensions obtained were freeze-dried to acquire dry nanopowders for inhalation at -40 ºC. For freeze-drying, Scanvac, Coolsafe 100–9 pro-type apparatus (LaboGeneApS, Lynge, Denmark) was used. Trehalose (5 % v/v) was used as a cryoprotectant. The other drying technique used was spray drying. For this purpose, a Büchi nano spray dryer (B90 HP Büchi, Switzerland) was used. The inlet temperature, outlet temperature, and peristaltic feed pump rate were set at 120 °C, 40 °C, and 20 % respectively. Mannitol and I400 were used as excipients in the spray drying. 4 % mannitol was added as an excipient to the suspension to obtain INH-CS/HA nanopowder with mannitol (CSM) and INH-MC/HA nanopowder with mannitol (MCM). 2 % w/v I400 was added as an excipient to the suspension to obtain INH-CS/HA nanopowder with I400 (CSI400) and INH-MC/HA nanopowder with I400 (MCI400).

3.2.5. Morphological, micrometric investigation and characteristics of powder

Scanning electron microscopy (SEM) (Hitachi S4700, Hitachi Scientific Ltd., Tokyo, Japan) was employed for the morphological investigation of the nanopowders. The particle size, PDI, and zeta potential of the nanopowders were investigated using Malvern zeta sizer Nano ZS (Malvern instrument, UK).

3.2.6. Physico-chemical investigations

FTIR (Thermo Nicolet AVATAR 330, USA) was employed to retrieve FTIR spectra. Samples were compressed into discs with KBr powder using a force of 10 kN with a hydraulic tablet press (Specac Ltd., UK). A 256-scan interferogram was obtained after the analysis of discs in the wavenumber range of 400 to 4000 cm^{-1}, at 4 cm^{-1} resolution.

X-ray Powder Diffraction (XRPD) measurements were recorded with Bruker D8 advance X-ray powder diffractometer (Bruker AXS GmbH, Germany) with Cu radiation at λ=1.5406 Å. VANTEC-1 detector was used to obtain the diffractograms (3^o - 40^o 2Θ) at 40 mA. Samples were mounted on the glass substrate at 40 kV.

The thermal behavior of the nanopowders was demonstrated by using Mettler Toledo DSC 821e (Mettler Inc., Schwerzenbach, Switzerland). The samples, approximately 3-5 mg, were hermetically

sealed in the aluminium pans. The samples were heated in the range of 25 and 300 °C in an argon atmosphere at a heat flow rate of 5 °C/minute.

3.2.7. Encapsulation efficiency

To determine the % encapsulation efficiency (EE) of the NPs, an indirect method was used. For this purpose, the nanosuspensions were centrifuged at 15,000 g for 20 min. The obtained supernatant was analyzed spectrophotometrically at 264 nm (λmax for INH). The following equation was then used to calculate the % EE,

$$\%\mathrm{EE} = \frac{\textbf{Total drug} - \textbf{free drug}}{\textbf{Total drug}} \times 100 \qquad [1]$$

3.2.8. Drug release and permeation studies

The release studies of the nanopowders were performed in the modified paddle method in the USP dissolution apparatus (SR8 plus dissociation test station, Hanson Research). All the studies were done in the simulated lung fluid. 10 mg INH and nanopowders equivalent to 10 mg drug were dispersed in 100 ml SLF at 37 ºC with 100 rpm rotation. After predetermined time intervals, 5 ml of the samples were withdrawn and centrifuged at 16,500 g for 10 min. the obtained supernatant was spectrophotometrically analyzed at 264 nm using a UV-visible spectrophotometer (Jasco V-730, Budapest, Hungary). The permeation of the drug content was demonstrated by using a modified horizontal diffusion cell model (Grown Glass, New York). Phosphate buffer (pH 7.4) was used in the donor chamber and simulated lung fluid was used in the accepting chamber separated by an artificial membrane (Isopore^{TM} membrane filter, 0.45 µm). Nanopowders equivalent to 10 mg of INH were dispersed in the donor chamber. The diffusion area was designed to be 0.69 cm^2 and the volume of media was kept constant in both the chambers.

3.2.9. Aerodynamic profile and in silico studies

The aerodynamic profile of the nanopowders was evaluated by the Andersen cascade impactor (ACI) (Copley Scientific Ltd., Nottingham, UK). The aerodynamic profile corresponds to the MMAD and FPF. ACI complies with the Ph. Eur. 2.9.18 (European Pharmacopoeia, 2015). Furthermore, the best sample was chosen based on the results and evaluated using the next-generation impactor (NGI). NGI is stated as the standard method for the evaluation of particle size distribution in the pulmonary passageways. An optical method (microscope) was linked with NGI for the assessment of the settlement of NPs on each tray. Furthermore, the results obtained from ACI were employed in the *in silico* stochastic lung model. The analytical method determined the exhaled fraction of particles, and the particle fraction deposited in acinar and bronchial zone of lungs after inahaltion of powders. This numeric integrated system tracks the particles till deposition or exhalation and a large number of particles (usually 10^5) are tracked till exhalation.

3.2.10. Cytotoxicity studies

For this purpose, an MTT assay was performed on the A549 cell line and raw 264.7 cell line; and MTS assay was performed on human primary macrophages. For MTT assay, the cells were seeded

in the 96-well cell culture microplates. CS/HA and MC/HA-based nanopowders were added to the wells at different concentrations followed by an incubation period of 24 h at 37 ^{o}C followed by the addition of MTT. The optical density was detected by EZ READ 400 ELISA reader (Biochrom, Cambridge, UK) at 550 nm. For MTS assay, the primary cells were seeded on a 96-well microplate. After incubation of 24 h, the culture media was replaced with the different concentrations of the nanopowders and incubated for a further 24 h. Optical density was measured at 490 nm using a microplate reader (Synergy H1 Hybrid Multi-Mode, BioTek, Winooski, VT).

3.2.11. Blood compatibility study

The blood compatibility profile of the nanopowders was demonstrated by a hemolysis assay. Fresh blood from human donors was used. After washing the blood samples with phosphate buffer saline by centrifugation at 250 g for 5 min, the red blood cells pellet was obtained. The pellet was redispersed with phosphate buffer saline and the resulting suspension of cells was seeded on the 96-well plate. After an incubation period of 4 h and 24 h at 37 ^{o}C, the absorbance of the samples was read at 570 nm by using a microplate reader (Synergy H1 Hybrid Multi-Mode, BioTek, Winooski, VT).

3.2.12. Cellular uptake of nanopowders

The visual intracellular uptake of nanopowders was demonstrated through a confocal laser scanning microscope (Leica SP5, Mannheim, Germany). For this study, the cells were seeded onto the individual Lab-Tek® chambered #1.0 borosilicate cover glass system and incubated for 24 h. DAPI dye was used for nuclei staining for better visualization. Rhodamine-B (Rh-B) labeled nanoformulations were incubated with cells. Mounting media was added to each glass chamber to perform imaging.

3.2.13. Macrophage phenotype analysis

The primary human macrophages were cultured and incubated with nanopowders for 24 h. These cells were then resuspended in phosphate buffer saline and stained with antibodies (CD80-PE and CD83-APC) with incubation for 25 min at -4 ^{o}C in dark. After incubation, the cells were washed and kept on ice till the quantification study. The maturation markers' level was quantified by flowcytometry in a BD FACSCalibur cytometer. For analysis of data, flowing software (Cell imaging core, Turku Centre for Biotechnology) was used.

3.2.14. Tolerogenic activity of nanoformulations

2,3-Indoleamine dioxygenase (IDO) is an immunosuppressant enzyme responsible for the catabolism of tryptophan, essential to the growth of microorganisms and affecting the T-cell tolerance. The primary macrophages were seeded and incubated on the 48-well plate with different formulations. L-tryptophan was added to the plates at least 4 h before the end of the incubation period. Culture media was obtained after centrifugation of cells at 10,000 g for 5 min at room temperature and trifluoroacetic acid was mixed with this obtained culture media to precipitate cell debris. The

obtained supernatant was mixed with Ehrlich reagent and the absorbance of the samples was analyzed through a microplate reader at 490 nm.

3.3. Statistical analysis

All the results are expressed as mean ± standard deviation. GraphPad Prism v.6.01 software (GraphPad Software Inc., San Diego, CA, USA) was used for data analysis. 2-way ANOVA test in combination with Dunnett's multiple comparisons tests was used to present the difference between donor groups.

4. RESULTS

4.1. Quantification of polymer

The number of mannose groups on the polymer was found to be 212 ± 27 µM per gram of MC. Moreover, the thiol groups anchored to the MC were quantified to be 328 ± 11 µM per gram, and disulfide bonds were quantified to be 74 ± 21 µM per gram of MC.

4.2. QbD and DoE for optimization of nanosuspensions

Lean QbD software® was employed to perform the interdependency between the critical attributes. Based on this relation, the critical CQAs affecting the QTPPs were chosen. Similarly, the CQAs critically influencing CMAs and CPPs were also selected. The highly influential CMAs and CPPs were prioritized by using DoE using BB factorial design. Different formulations were prepared according to the number of experimental runs recorded by STATISTICA® 10 software and these runs were studied against the dependent outcomes such as size, PDI, and zeta potential (**Table 1**). This robust method was used for developing the nanosystem using CS polymer and was repeated with the same parameters for the MC-based systems due to the same origin of the polymer.

Table 1: *The results of dependent variables obtained through 15 runs by Box-Behnken design in STATISTICA®10 for CS/HA NPs*

Run codes	HA (mg)	CS (mg)	Sonication pulse ratio	Average size (nm)	PDI	Zeta potential (mV)
C1	6.5	2.5	30	390	0.417	30.5
C2	5.0	3.25	30	399	0.432	28.2
C3	2.5	1.25	40	324	0.202	27.8
C4	5.0	1.25	30	387	0.391	30.6
C5	5.0	2.5	40	342	0.199	34.3
C6	5.0	2.5	40	346	0.187	32.1
C7	6.5	3.25	40	457	0.451	28.5
C8	5.0	1.25	50	363	0.215	29.8
C9	2.5	3.25	40	398	0.331	28.5
C10	6.5	1.25	40	375	0.411	31
C11	2.5	2.5	30	330	0.216	19.5
C12	5.0	3.25	50	390	0.185	27.9
C13	5.0	2.5	40	351	0.214	28
C14	2.5	2.5	50	308	0.204	22.2
C15	6.5	2.5	50	415	0.398	27.5

The encapsulation efficiency for the freeze-dried and spray-dried samples was quantified. The size, PDI and % EE of the optimized freeze-dried and spray-dried nanopowders (Table 2). As presented, a significant difference in the % EE was observed among the freeze-dried and spray-dried samples. However, no significant change in particle size was observed based on the drying techniques.

Table 2: *The size, PDI, zeta potential, and % EE of the optimized nanopowders*

Parameters	MCM	MCI400	MC/HA	CSM	CSI400	CS/HA
Average size (nm)	316 ± 25	323 ± 15	302 ± 11	404 ± 10	299 ± 19	300.2 ± 11
Zeta potential (mV)	21.4 ± 4.01	14.5 ± 0.93	31.2 ± 2.35	18.4 ± 6.01	24.1 ± 5.50	30.1 ± 3.13
PDI	0.215 ± 0.91	0.398 ± 1.5	0.211 ± 2.89	0.246 ± 0.07	0.310 ± 1.01	0.204 ± 0.01
Encapsulation efficiency (%)	74.05 ± 8.22	63.45 ± 2.84	90.17 ± 1.01	72.43 ± 2.41	59.66 ± 1.84	91.21 ± 2.31

4.3. Morphological investigation of powder

As shown in **figure 2**, the freeze-dried nanopowders did not present smooth-surfaced morphology. Also, the freeze-dried samples had patches of aggregation. On the other hand, the spray-dried samples with mannitol demonstrated smooth mono-dispersed particles. However, using I400 yielded particles with aggregated appearance.

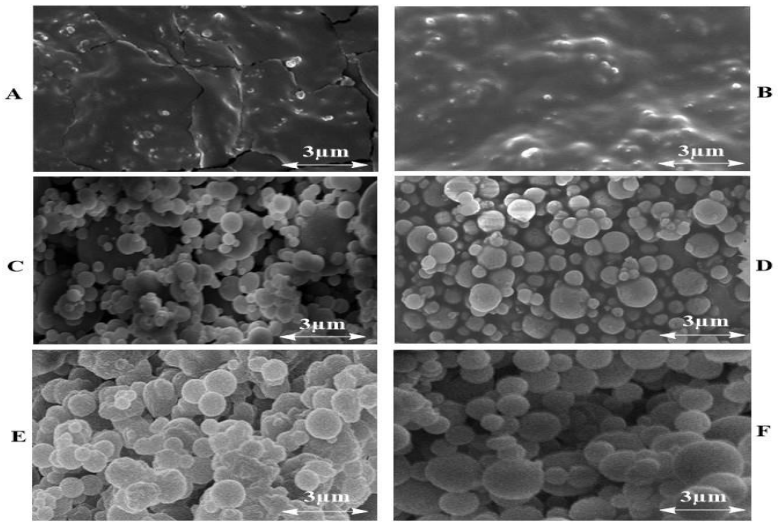

Figure 2: *Scanning electron microscopy (SEM) micrographs of the freeze-dried and spray-dried nanopowders. (A) CS/HA NPs, (B) MC/HA NPs, (C) CSI400, (D) CSM, (E) MCI400 and (F) MCM.*

4.4. Outcomes of physicochemical investigation

FTIR experiment demonstrated the compatibility between the components of the freeze-dried and spray-dried nanopowders (**Figure 3**). The loaded drug INH displayed the characteristic peaks at 3000-3300 cm^{-1}. All the corresponding peaks of CS, HA, MC, mannitol, and I400 were found to be

present at 1600 cm^{-1}, 1400 c^{-1}, 1200 cm^{-1}, 3300 $cm^{-1,}$ and 1200 cm^{-1} in the FTIR peaks of samples respectively.

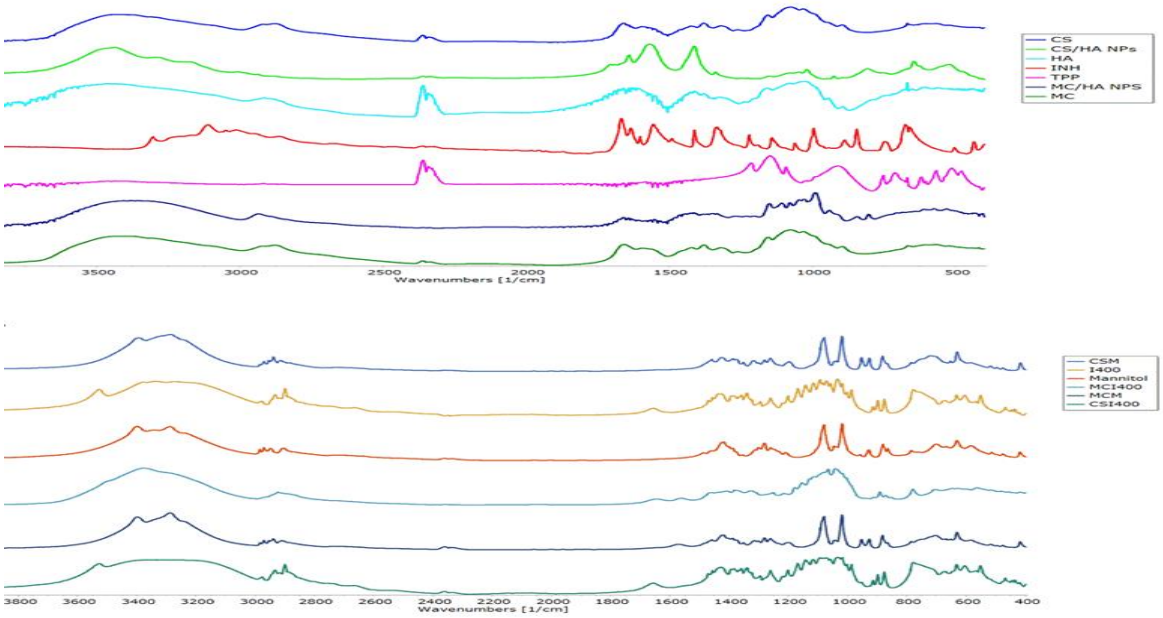

Figure 3: *IR spectra of (A) freeze-dried and (B) spray-dried nanopowders*

The XRPD images (**Figure 4**) of freeze-dried and spray-dried samples did not exhibit any discrete crystalline peaks that were initially present in the nascent INH between 10º and 40º. Mannitol and I400 existed as a crystalline excipient before and after the drying process.

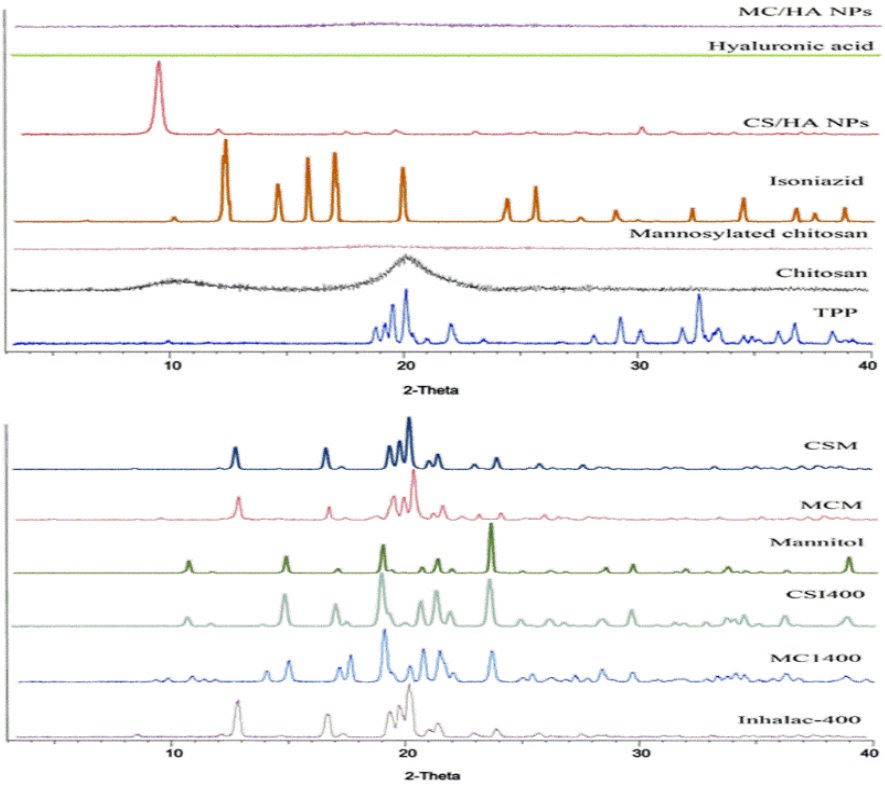

Figure 4: *XRPD diffractogram of freeze-dried and spray-dried nanopowders*

The Differential Scanning Calorimetry (DSC) curves (**Figure 5**) presented the absence of the melting point of INH in all the samples Mannitol-based samples exhibited an endothermic peak at 169 ºC showing the melting of the mannitol during the drying process.

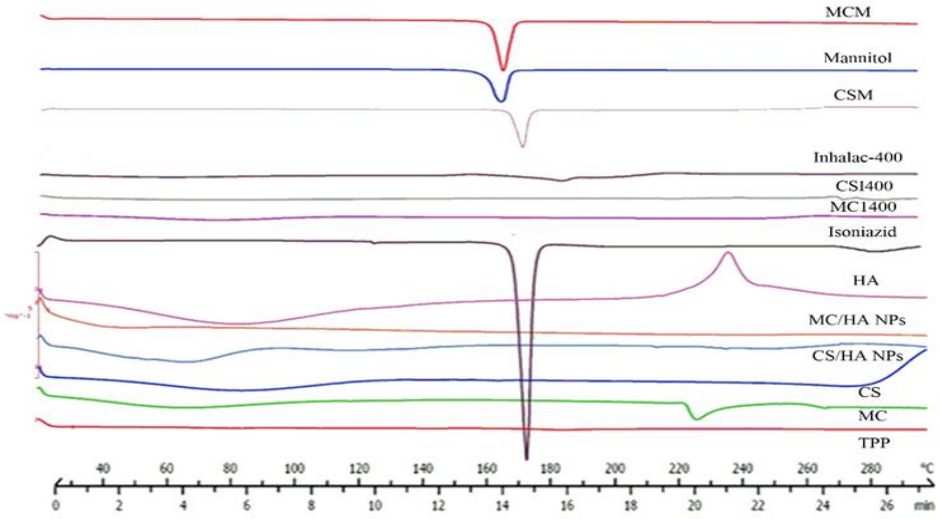

Figure 5: *DSC curves for the freeze-dried and spray-dried nanopowders, Exo ↑ (b)*

4.5. Drug release and permeation study outcomes

It can be observed from **Figure 6,** that the release of INH was slowed down as the polymeric composition changed from CS to MC, 63% to 40 %, demonstrating that mannosylation facilitates the controlled release. However, there was no significant change in the release patterns of INH from the spray-dried and freeze-dried samples. Approximately 58-72 µg/cm^2 of INH was able to permeate across the membrane filter into the acceptor phase in 2 h, for the MC-based samples irrespective of the drying technique (**Figure 7**). A slight visible difference was observed in the permeation pattern of INH from the CS-based nanopowders, with a maximum concentration of 46-48 µg/cm^2 for CSM.

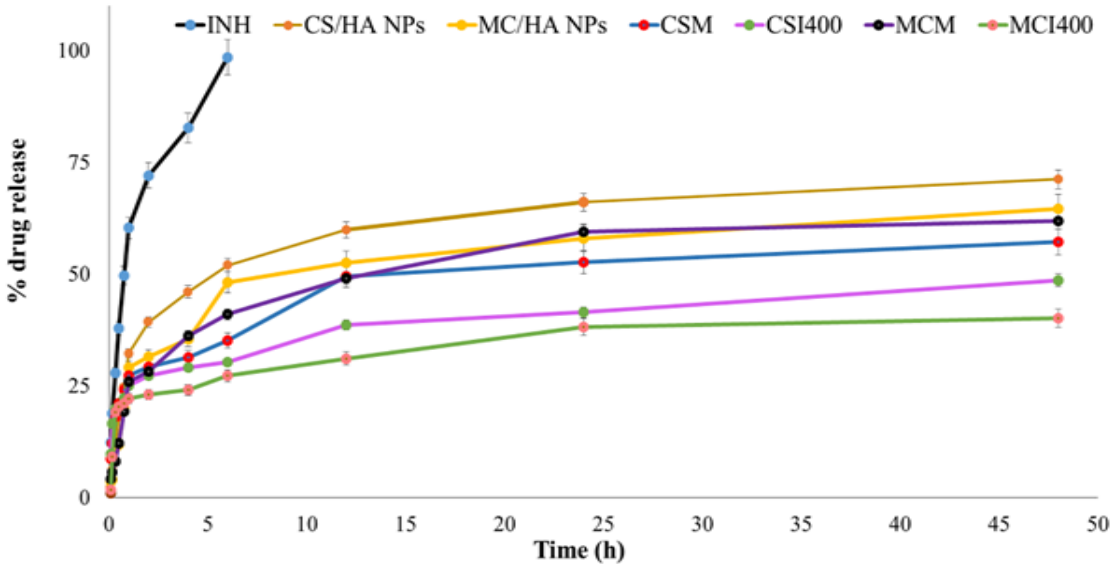

Figure 6: *The in vitro release of INH from freeze-dried and spray-dried nanopowders, in the simulated lung media (pH 7.4)*

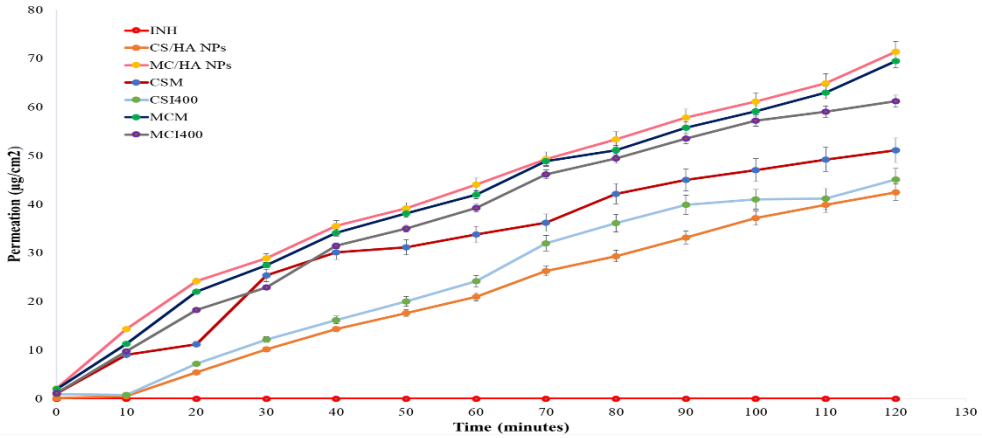

Figure 7: *The in vitro permeation profile of INH (µg/cm^2) from the freeze-dried and spray-dried nanopowders from donor to acceptor chamber.*

4.6. Aerodynamic profile and *in silico* modeling

The aerodynamic profile as investigated by ACI presented the favorable MMAD of the nanopowders (**Table 3**). MMAD values for freeze-dried nanopowders, CS/HA NPs, and MC/HA NPs were found to be 2.67 µm and 2.981 µm respectively. Similarly, the MMAD for the spray-dried nanopowders ranged between 1.632 µm - 3.556 µm. The particles below the range of 3 µm have a higher tendency to deposit in the bronchial as well as the alveolar region (FPF < 3 µm). Later, the best sample (MCM) was chosen for the evaluation in terms of mass size distribution and the results were fetched based on the surface coverage of the collection plates. The data presented that the average mass size distribution of more than 50 % of the particles had a size of 1.37 - 2.3 µm.

Table 3: *The aerodynamic parameters of freeze-dried and spray-dried samples as determined by ACI*

Parameters	MCM	MCI400	MC/HA	CSM	CSI400	CS/HA
MMAD (µm)	1.632 ± 0.11	2.464 ± 0.23	2.981 ± 0.12	3.556 ± 0.24	2.891 ± 0.09	2.67 ± 0.05
FPF <5 µm (%)	80.94 ± 0.66	74.89 ± 0.16	69.01 ± 0.05	62.73 ± 1.8	68.94 ± 0.19	62.11 ± 1.06
FPF <3 µm (%)	69.46 ± 0.97	59.14 ± 1.11	50.11 ± 0.18	44.04 ± 0.19	50.91 ± 0.61	68.70 ± 0.11

According to *in silico* studies as shown in **figure 8**, approximately, 30 % of the nanopowders were deposited in the extra-thoracic region for all the freeze-dried samples irrespective of breath-hold time. On the contrary, the results varied for the extra-thoracic fraction of spray-dried samples in the range of 14 - 41 %. Similarly, the exhaled fraction was presented to be higher in the case of spray-dried samples, especially for I400-based nanopowders. However, MCM demonstrated better aerodynamic characteristics in the model, by presenting a low exhaled fraction with a high extra-thoracic fraction than all the other spray-dried nanopowders, by increasing breath-hold time.

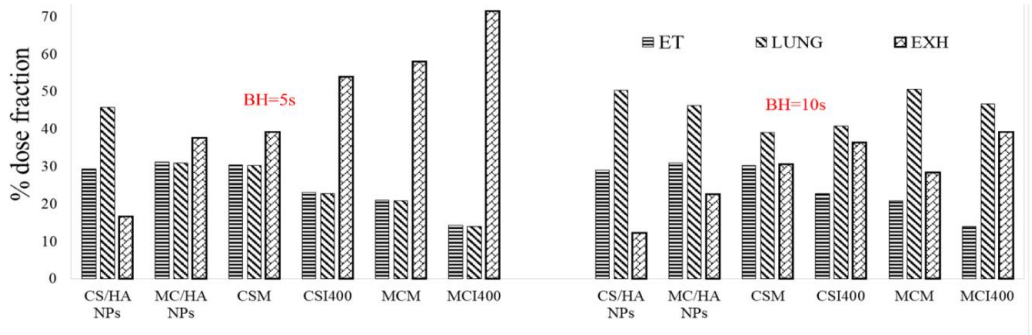

Figure 8: *Presentation of in silico deposition modeling at two breath-hold (BH) times, for the freeze-dried and spray-dried nanopowders. [ET: fraction of the nanopowder deposited in the extra-thoracic airways, LUNG: cumulative fraction of nanopowders deposited in the bronchial and acinar region, EXH: exhaled fraction of the nanopowders].*

4.7. Overview of cytotoxicity studies

For the A549 cells, almost all the samples demonstrated the viability of more than 80 %, and MC-based nanosystems exhibited up to 100 % viability of cells (**Figure 9A**). On the contrary, the cytotoxicity of the nanosuspensions on the Raw 264.7 macrophages was found to be concentration-dependent. The low concentrations of INH, i.e., 0.5 mg/ml and 0.01 mg/ml exhibited more than 50 % cell viability but it was cytotoxic to the Raw 264.7 macrophages at high concentrations (**Figure 9B**).

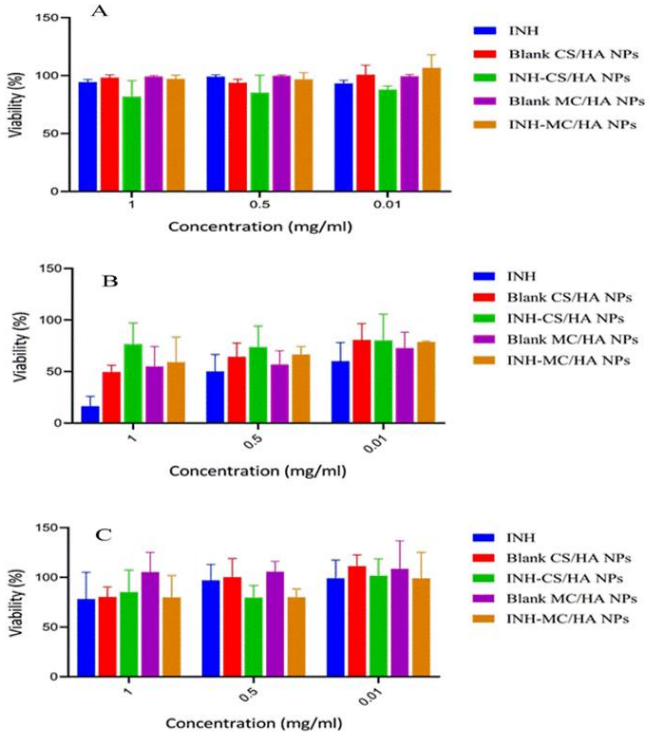

Figure 9: *The percentage viability of nanosuspensions on (A) A549 cells, (B) Raw 264.7 macrophages, and (C) primary human macrophages, after an incubation period of 24 h for different concentrations (0.01, 0.5, 1 mg/ml). All the results are expressed as mean ± S.D, n=3*

Likewise, the cytotoxicity studies on the primary human macrophages derived from human blood highlighted similar behavior (**Figure 9C**). The results were evidently but not primarily dependent on

the increase in the concentration. Furthermore, almost all the results were promising and presented viability of ≥ 70 %.

4.8. Evaluation of blood compatibility study

According to ISO/TR 7406, the safe hemolytic ratio for the biomaterials is considered to be less than 5 %. All the nanosuspensions were found to be hemocompatible in the case of this study (**Figure 10**) where none of the samples posed any visible lytic effect on RBCs, irrespective of the incubation period.

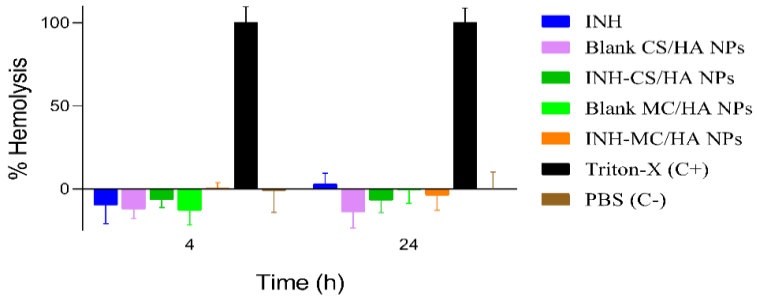

Figure 10: *Blood compatibility study performed on fresh human blood, after 4 h and 24 h. The results are expressed as mean ± SEM, with the results from three different blood donors.*

4.9. Demonstration of cellular uptake of nanopowders

As it can be seen from **figure 11**, there is a shift in fluorescence intensity after the internalization of NPs inside the cells as compared to the untreated control. The uptake of Rh-B CS/HA NPs was relatively lower in A549 cells and Raw 264.7 macrophages as compared to Rh-B MC/HA NPs. Macrophages are the immune cells responsible for phagocytosis and are more responsive to the uptake of NPs as compared to alveolar epithelial cells. The study was performed on A549 cells based on the fact that NPs interact with alveolar epithelial cells before engulfment by macrophages.

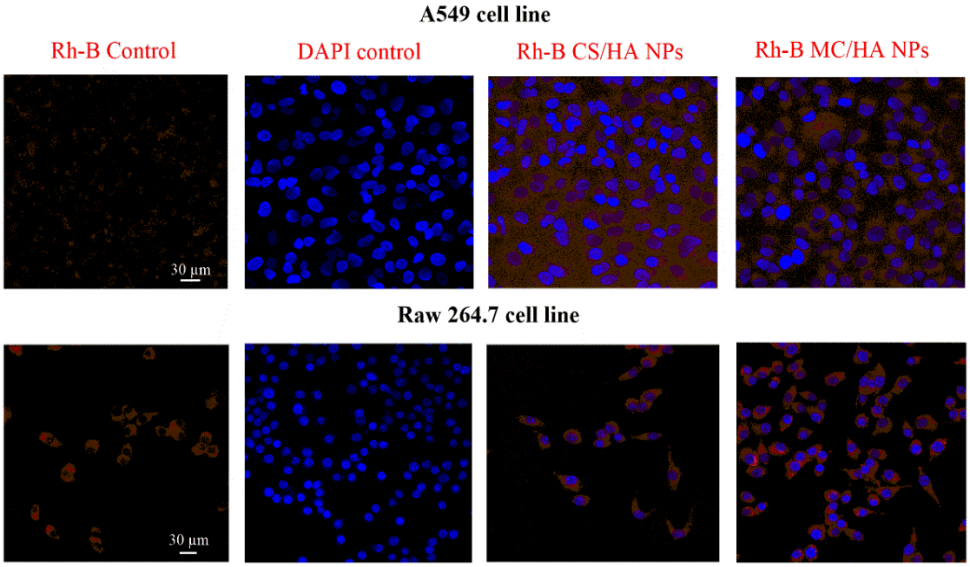

Figure 11: *Nanoparticulate uptake study by confocal laser scanning microscopy after an incubation period of 2 h. The red color indicates the fluorescence due to Rhodamine-B dye (Excitation λ_{max}= 546 nm, Emission λ_{max}= 568 nm) and the blue color is indicated the fluorescence due to DAPI-nuclei dye (Excitation λ_{max}= 359 nm, Emission λ_{max}= 457 nm)*

4.10. Overview of macrophage phenotype analysis

T-lymphocyte costimulatory molecules (CD80 and CD83) are the indicators of pro-inflammatory macrophage-activated phenotype. CD80 is also responsible for the expression of interleukin-6 which is involved in the resistance against TB due to its pro-inflammatory nature. Likewise, CD83 levels elevate in the activated macrophage. There is an alleviation of inflammation due to the inhibition of CD83. Altogether, the results (**Figure 12**) demonstrated the upregulation of the maturation markers and hence the T-cell activation essential to the immune regulation in TB.

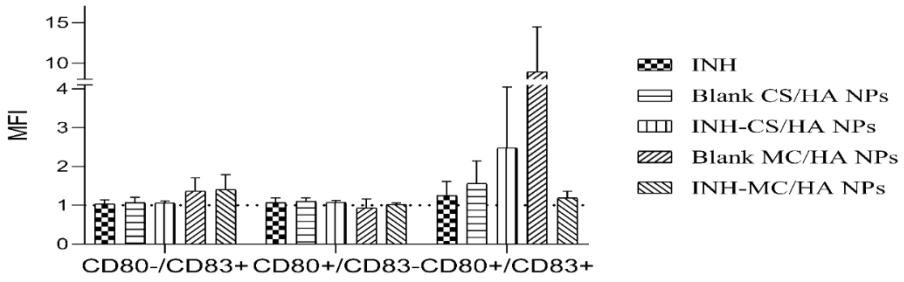

Figure 12: *The expression of macrophage maturation markers, CD80 and CD83 as % quantified. The dotted line represents MF=1, which indicates the signal from the incubated macrophages in culture. All the results have been expressed as mean MFI ± SEM, n=blood from 3 donors*

4.11. Determined tolerogenic activity of nanoformulations

Macrophages can affect immune regulation and peripheral tolerance by the IDO expression. Hence, IDO activity was tested by the incubation of nanosuspensions with macrophage cultures (**Figure 13**). It is noteworthy that the tolerogenic response suppresses immune regulation in TB. Interestingly, there was no tolerogenic response recorded for the nanosuspensions similar to that of control (macrophages in culture media).

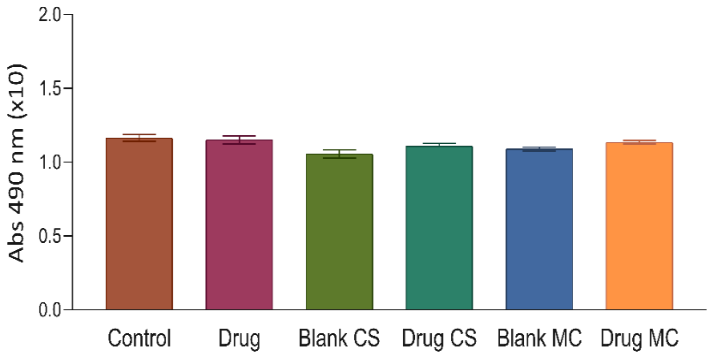

Figure 13: *Evaluation of the 2,3-Indoleamine dioxygenase (IDO) after the incubation of nanosuspensions with human macrophage culture*

5. CONCLUSION

Already marketed dosage forms fail to deliver the drug to the target site where the causative bacteria reside. Therefore, an adequate drug dose has to be administered to maintain the therapeutic concentration at the target site which however leads to toxicity and drug resistance over time. Hence, this work aimed to deliver the anti-tubercular to the target site to achieve consistent therapeutic outcomes.

1. The polymers employed in this work were selected based on their affinity for the macrophages.
2. QbD was implemented to identify the CQAs, CPPs, and CMAs critical to the QTPPs for the preparation of nanosuspensions. Optimization was carried out using time-saving robust DoE that gave an output of the experimental runs to identify the most rational concentrations of polymers. The optimal concentrations of the HA and CS/MC were found to be 5 mg and 2.5 mg respectively. 10 % of the oral dose was encapsulated in the NPs, as established by the literature. And, the sonication speed for the homogenous mixing of the nanosuspension was selected to be 50 pulses per minute.
3. The ionic gelation method was employed for the synthesis of nanosuspension which is a very cost-effective and time-saving nanosuspension synthetic approach. Also, Spray-drying and freeze-drying were utilized to obtain the dry nanopowders for inhalation. The PDI for the freeze-dried nanopowders was approximately 0.2 which revealed the highly uniform and narrow size distribution. The results were different in the case of spray-dried nanopowders. Mannitol-based samples were homogenous with the PDI values less than 0.25. Unlikely, the use of Inhalac® 400 presented the aggregation in the samples due to the hygroscopic nature of the excipient. The average particle size was 300 nm for the freeze-dried nanopowders. However, the particle size varied within the range of 299 to 404 nm for the spray-dried samples. The zeta potential values were high for all the nanopowders irrespective of the drying technique.
4. All the *in vitro* characterization approaches demonstrated the compatibility among the excipients, polymers, and drug. The aerodynamic parameters of the nanopowders were highly promising in the case of spray-dried MCM with an MMAD of 1.632 and FPF < 5 µm of 80 % among all the samples.
5. The nanosystems were found to be biocompatible, hemocompatible, and posed no toxicity to the cells based on the *ex vivo* studies. No immune-suppressive response was exhibited during the studies. The T-lymphocyte costimulatory markers CD80 and CD83 were upregulated in the macrophage phenotype study which highlighted the T-cell activation upon the contact of nanosystems to macrophages.

6. NOVELTY AND PRACTICAL ASPECTS

1. A pulmonary inhalation system developed using nanotechnology combined the promising attributes of nano-dimensional powders and inhalation in a targeted approach toward macrophages in the lungs.

2. The novelty of this work is based on the aspect that all the preliminary regulatory aspects were also explored apart from the pharmaceutical concerns. The thorough literature review gave an insight into the critical aspects of formulation development followed by QbD rational designing.

3. The method used was cost-effective along with the low cost of natural polymers. The lyophilized powders for injection are already on the market and hence this freeze-dried approach can easily be scaled-up for the pulmonary administration. Moreover, the pulmonary powders available in the pharmaceutical industry employ spray-drying currently. Therefore, both drying approaches can be practical in terms of R&D.

PUBLICATIONS RELATED TO THE SUBJECT OF THE THESIS

1. **Mukhtar Mahwash**, Hussain Ali, Naveed Ahmed, Rashid Munir, Sumbal Talib, Anam S. Khan, and Rita Ambrus. "Drug delivery to macrophages: A review of nano-therapeutics targeted approach for inflammatory disorders and cancer." *Expert Opinion on Drug Delivery* 17(9) (2020): 1239-1257.

(Q1)

2. **Mukhtar Mahwash**, Edina Pallagi, Ildikó Csóka, Edit Benke, Árpád Farkas, Mahira Zeeshan, Katalin Burián, Dávid Kókai, and Rita Ambrus. "Aerodynamic properties and *in silico* deposition of isoniazid loaded chitosan/thiolated chitosan and hyaluronic acid hybrid nanoplex DPIs as a potential TB treatment." *International Journal of Biological Macromolecules* 165 (2020): 3007-3019.

(Q1)

3. **Mukhtar Mahwash**, Eszter Fényes, Csilla Bartos, Mahira Zeeshan, and Rita Ambrus. "Chitosan biopolymer, its derivatives and potential applications in nano-therapeutics: A comprehensive review." *European Polymer Journal* 160 (2021): 110767.

(Q1)

4. **Mukhtar Mahwash**, Zsolt Szakonyi, Árpád Farkas, Katalin Burian, Dávid Kókai, and Rita Ambrus. "Freeze-dried vs spray-dried nanoplex DPIs based on chitosan and its derivatives conjugated with hyaluronic acid for tuberculosis: *In vitro* aerodynamic and *in silico* deposition profiles." *European Polymer Journal* 160 (2021): 110775.

(Q1)

5. **Mahwash Mukhtar**, Noemi Csaba, Sandra Robla, Rubén Varela-Calviño, Attila Nagy, Katalin Burian, Dávid Kókai and Rita Ambrus. "Dry powder comprised of isoniazid loaded nanoparticles of hyaluronic acid in conjugation with mannose anchored chitosan for macrophage targeted pulmonary administration in Tuberculosis." *Pharmaceutics* (under review).

(Q1)

6. Ildikó Csóka, Keyhaneh Karimi, **Mahwash Mukhtar**, and Rita Ambrus. "Pulmonary drug delivery: Role of antibiotic formulations for treatment of respiratory tract infections".*Acta Pharmaceutica Hungarica* 89(2) (2019): 43-62.

(Q4)

PRESENTATIONS RELATED TO THE THESIS

1. **Mahwash Mukhtar** and Rita Ambrus. “Fabrication of pulmonary formulations containing hyaluronic acid and chitosan-based nanoparticles for drug delivery in tuberculosis”. I-Symposium of Young Researchers on Pharmaceutical Technology, Biotechnology and Regulatory Science. p. 5. (2019)

2. **Mahwash Mukhtar** and Rita Ambrus. “Development of Inhalable Chitosan nano system conjugated with Hyaluronic acid for treatment of Tuberculosis”. II-Symposium of Young Researchers on Pharmaceutical Technology, Biotechnology and Regulatory Science. p. 38. (2020)

3. **Mahwash Mukhtar** and Rita Ambrus. “Fabrication of isoniazid loaded chitosan/thiolated chitosan and hyaluronic acid hybrid nanoplex DPIs as a potential TB treatment: Aerodynamic properties and *in silico* deposition in lungs”. EUGLOH Annual Student Research Conference (2020)

4. **Mahwash Mukhtar** and Rita Ambrus. “A Design of Experiment (DoE) approach for the chitosan/thiolated chitosan and hyaluronic nanoplexes for the pulmonary drug delivery in tuberculosis”. Medical Conference for PhD Students and Experts of Clinical Sciences. p. 38. (2020)

5. **Mahwash Mukhtar** and Rita Ambrus. “Spray dried hyaluronic acid nanoplexes conjugated with chitosan and its derivatives for the pulmonary administration as dry powder inhalers for tuberculosis”. III-Symposium of Young Researchers on Pharmaceutical Technology, Biotechnology and Regulatory Science. p. 16. (2021)

6. **Mahwash Mukhtar** and Rita Ambrus. “*In silico* and *in vitro* aerodynamic profile of chitosan/thiolated chitosan and hyaluronic acid hybrid nanoplex based DPIs for tuberculosis”. Journal of aerosol medicine and pulmonary drug delivery 34(3) pp. A11-A12. DOI: 10.1089/jamp.2021.ab01.abstracts (2021).

7. **Mahwash Mukhtar**, Noemi Csaba, Sandra Robla and Rita Ambrus. “Mannosylated chitosan-based pulmonary drug delivery system for targeting macrophages”. IV-Symposium of Young Researchers on Pharmaceutical Technology, Biotechnology and Regulatory Science. p. 28. (2022).

This work was supported by the Stepindium Hangaricum Programme, Ministry of Human Capacities, Hungary, grant number 20391-3/2018/FEKUSTRAT, and Gedeon Richter Ltd –GINOP project (2.2.1-15-2016-00007), GINOP-2.3.2-15-2016-00036 (Development and application of multimodal optical nanoscopy methods in life and materials sciences) and Project No. TKP2021-EGA-32 is financed under the TKP2021-EGA funding scheme. I am grateful to my supervisor Dr. Rita Ambrus and my co-authors for their help and support throughout my Ph.D. studies.